

WORK DEVELOPMENT IN THE MUSCLES OF THE JUMPING FROG

By

Steven S. Saliterman

SUBMITTED IN PARTIAL FULFILLMENT FOR THE DEGREE

SUMMA CUM LAUDE

IN THE COLLEGE OF LIBERAL ARTS,

UNIVERSITY OF MINNESOTA

JUNE 25, 1973

Work Development in the Muscles of the Jumping Frog

Abstract

The energy expended as work by a frog when it jumps can be accurately and easily measured with the Laser Activated Amphibian Monitor System (LAAMS). The motion of the center of mass of a frog in flight is fully understood. This includes an analysis of air resistance and the resulting drag. Several equations are described that have application with both LAAMS and the former photographic techniques used to study frog jumping. These equations when used with LAAMS require computer manipulation. The required computer program is described in detail.

The advantage of LAAMS over former techniques and its potential as an investigative tool will become evident as our story of work development leaps forward!

Introduction

Power development is defined as the total energy expended divided by the product of muscle mass and the time over which the energy was expended.

$$PD = ET / (MM \times TA)$$

In the frog MM is the mass of the muscles that contract in the hind limb when the frog jumps. The time of acceleration or TA is the time interval beginning with the first sign of force against the ground to the instant the distal phalanges leave the ground.

The recently developed Laser Activated Amphibian Monitor System (LAAMS) allows for easy and rapid measurement of work development.

$$WD = EW / (MM \times TA)$$

The energy expended as work, EW, is the sum of kinetic energy and unrecovered potential energy expended by the frog as it jumps. As we will see later, power development and work development are closely related.

By forcing the frog to jump several times within a short time period, a work development decay curve can be constructed. In future experiments several frogs (chosen for similarity of certain characteristics) will be divided into control and experimental groups. Differences in work development decay curves found between groups (each frog in each group makes several jumps) may be attributed to effects of the experimental variable. Choice of the experimental variable is almost unlimited. For example, the effect of selected drugs on the functioning of the muscles might be monitored via work development measurements. Other variables include temperature, air composition, the frogs diet and even the sex and age of the frog. Moreover, differences in work development between different species of frogs and toads can be observed, as well as seasonal and regional variations within a given species. An understanding of these "natural variables" is important if an accurate analysis of the effects of artificial variables is to be accomplished.

Power development and work development are related by way of the mechanical efficiency of muscle. The total energy spent by muscle during contraction is the sum of work and heat energy.

$$ET = EW + EH$$

The mechanical efficiency of muscle is the ratio of the work performed by muscle to the total energy spent (1).

$$\text{efficiency} = EW / ET$$

The total amount of heat liberated when muscle contracts has been the center of considerable controversy. Hill (2,3,4,5) contends that when muscle contracts energy is liberated in three forms: 1.) A, heat of activation, 2.) heat of shortening, ax , and 3.) the mechanical work EW.

$$ET = EW + A + ax$$

The amount of shortening is x , and a is a constant. In a tetanic contraction the heats of activation due to successive stimuli are together known as the maintenance heat. Carlson, Hardy and Wilkie (6) believe that shortening heat as such does not exist. Their technique for measuring total energy output is based on measurement of phosphocreatine hydrolysis. Phosphocreatine hydrolysis did show a constant term that corresponds to A above and a linear term that corresponds with EW. If the total quantity of heat liberated during a frog's jump could be measured, then an accurate power development figure would be obtained. Since heat can be measured in the isolated muscle, approximate values for muscle efficiency can be obtained. Multiplying the reciprocal of efficiency of the hind leg muscle system times the work development will give the power development.

$$PD = (1 / \text{efficiency}) \times WD$$

The power development decay curve of a frog forced to jump several times consecutively is representative of the decrease in available chemical energy for muscle contraction. Once significant differences are obtained between a control group and an experimental group of frogs, the next task is to account for why the differences occur. The ultimate explanations center around variances in the normal biochemical processes of muscular contraction. An understanding of the "normal processes" has only recently come to light-and much remains to be explained. The mechanism of contraction has been carefully studied by Huxley (7).

The work of Maruyama and Weber (8) on the binding of ATP to myofibrils is representative of biochemical studies that are beginning to bring the process of contraction into focus.

Previous Works on Frog Jumping

Although work development in the jumping frog has been previously unexplored, many attempts have been made to relate the distance an amphibian jumps to physical dimensions of the animal. Rand and Rand (9,10) have determined that the total body length of *Bufo Marinus* varies with the cube root of the weight and with the hind limb length. Moreover, they have also shown that the distance jumped varies directly with the hind limb length. Stokely and Berberian (11) were unable to conclude that "changes in the relative proportions of the skeletal parts of the frog hind leg appreciably influence jumping ability." Gans and Rosenberg (12) determined a linear relationship between body weight of *Bufo Marinus* and the estimated force exerted when the animal jumps. (Gans and Parsons (13) have given a rather interesting analysis on the origins of the jumping mechanism in frogs).

Gray's work on animal locomotion, Hirsch's work on the mechanism of frog jumping, and E.C.B. Hall-Cragg's analysis of the jump of the Lesser Galago are perhaps the most useful works in regard to work development in the muscles of the jumping frog. Gray (14,15) in his discussion of amphibian jumping correctly describes the movement of the center of mass of the frog from the time it is in flight to the instant it touches the ground. His mathematical interpretation of the event is however extremely limited. Nevertheless, his photographs do clearly show the orientation of the limbs during flight. Hirsch (16) has done an excellent analysis of the acceleration phase. Figure 1 shows the form of the frogs acceleration. Figure 2 shows from a side and top view the orientation of the limbs during the various stages of figure 1. The drawings in figure 1 were made by Hirsch via high speed photography. Former techniques used to measure the initial velocity of a jumping frog consisted of measuring the path over which the frog accelerated and the time spent accelerating. Unfortunately this is an extremely inaccurate procedure. The actual path taken by the center of mass can only be estimated. In addition, the acceleration is not uniform and leads to complications when trying to determine the initial velocity. Nevertheless, photographs do give an accurate

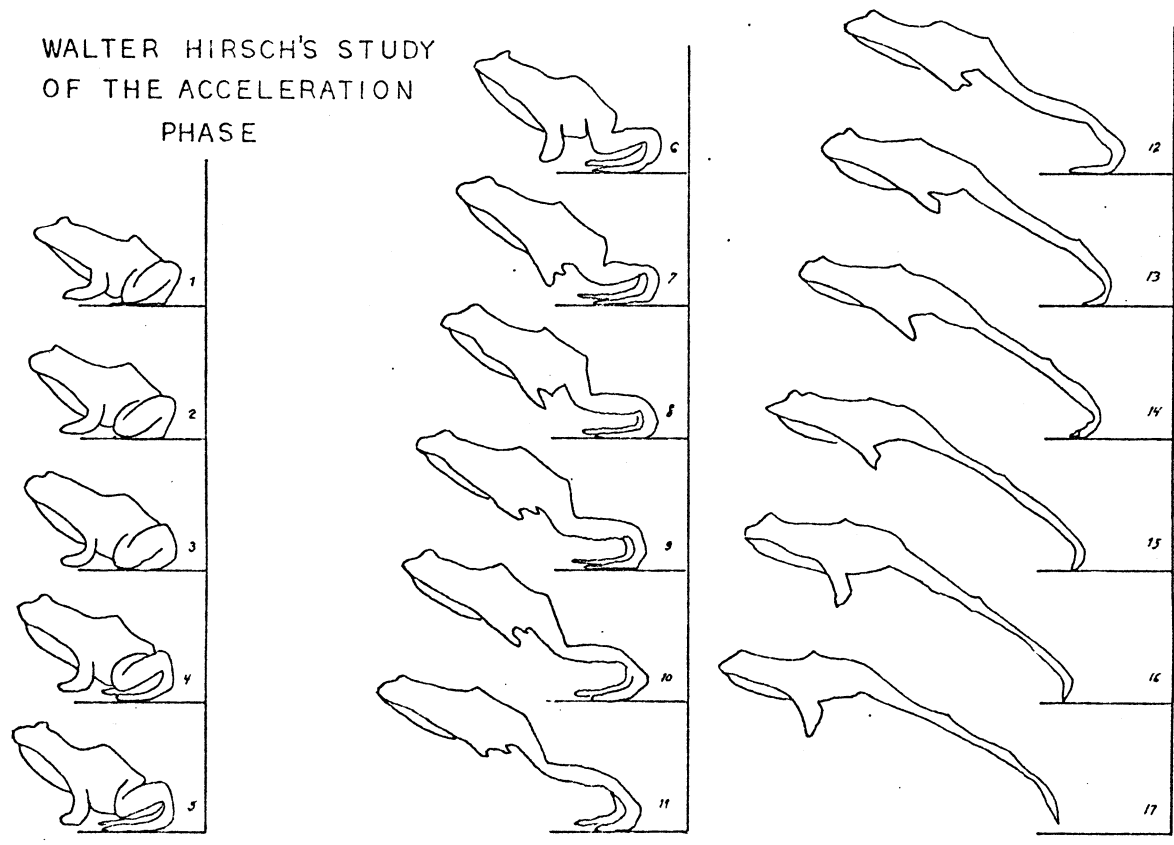


Fig. 1. The spring-like thrust of acceleration is easily seen in Hirsch's high-speed photographs of the jump.

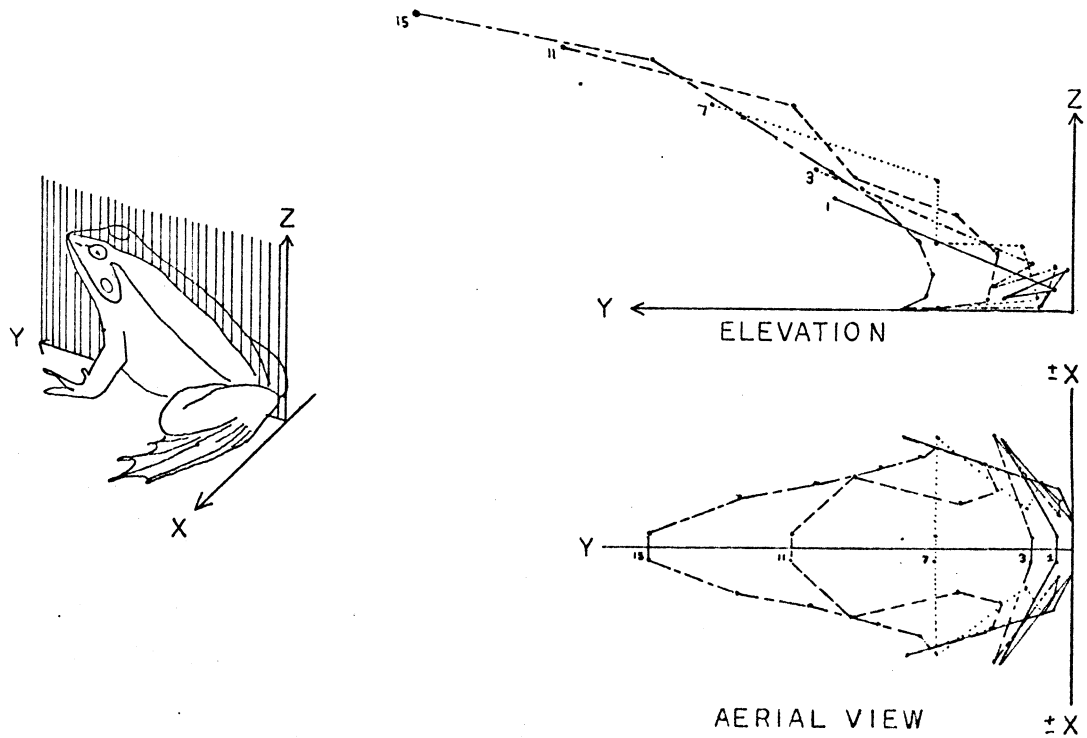


Fig. 2. These side and aerial views of the bones and joints during the acceleration phase correspond with the individual frames of figure 1. The corresponding bones from the pelvic girdle downward are the femur, tibio-fibula, astragalus/calcaneum, metatarsal and phalanges. (A complete discussion on the bones and muscles of the hind limb can be found in Dr. Alexander Ecker's The Anatomy of the Frog, Oxford, 1889).

measure of the angle of trajectory. Developing photographs for each jump of an entire experiment consisting of many frogs and many jumps would be expensive and time consuming. LAAMS is capable of electronically measuring all the parameters of an amphibian jump on a real time basis. No assumptions are made about the acceleration, and air resistance may be included into the calculations.

Hirsch's work paired with Zugs (17) work on the relation between jumping and osteometrics may eventually allow for calculation of the change in length individual muscles undergo during the acceleration phase. Given work development of a particular jump the technique used by E.C.B. Hall-Craggs can be used to determine the force and tension developed in individual muscles. This technique consists of determining the force each muscle must apply to given joints so that the resultant of all forces produces the final measured force. Given Hirsch's side and top views of the limb orientation as acceleration proceeds, the angular velocity with which the various joints "open up" may be calculated. This would allow for calculation of the velocity of shortening of individual muscles. Admittedly the above argument needs considerable modification and evaluation before ever being attempted. It is presented however to show that energy relationships in the living animal should not be passed off as impossible items to measure. If velocity, tension, and length of individual muscles in the accelerating frog are determined, then it may be possible to construct a three-dimensional representation of the chemical energy available for contraction. (18)

LAAMS

The Laser Activated Amphibian Monitor System is designed to measure the time spent accelerating, time in flight, and the final horizontal displacement of the center of mass of a jumping frog. This data paired with measurements taken from a simple center of mass exercise can be used to generate the initial velocity (V_0) and initial angle of takeoff (θ_0). In addition, as seen in figures 7, 8 and 9, the following information can be calculated:

- 1) θ_w = reentry angle
- 2) V_w = reentry velocity
- 3) Most of the labeled segments (some are measured)
- 4) Potential energy
- 5) Kinetic energy
- 6) Work development
- 7) Approximate power development
- 8) Drag

An explanation of the various segments, points and other parameters, as well as the necessary equations for their solution will be discussed in the next section.

The LAAMS is best described by the flowchart of figure 3. The system consists of three main units--a large, long and narrow plexaglass tank (figure 4), a automatic temperature controller that maintains the tank air temperature at a predetermined level (10°c - 50°), and a photocell decoder.

The three units interact in the following way. An experiment is selected and the necessary frogs are obtained. The tank's atmospheric composition, temperature, and lighting are then set to conform with the experiment's requirements. (atm. pressure must not deviate by more than approximately 25 mm Hg from the external pressure). A frog is chosen and placed inside the tank on top of the platform shown in figure 4. This platform is in reality a tread that will automatically bring the frog to the "zero line" whenever the frog is at rest and away from the zero line. In other words, after the frog jumps it is brought back to the beginning point automatically.

The laser provides two planes of light that are planar with the platform. One is located even with the tread and is normally blocked or "off" when the frog is at rest. The other plane is located just above the frog's head (it is adjustable) and is normally "on" when the frog is at rest. The planes are in reality each composed of a continuous laser beam that is bounced back and forth on end mirrors, giving in effect "planes" of light. A top and side view of this arrangement is shown in figure 5. The two starting beams for each plane are derived by splitting a single He-Ne laser beam. The beams, after being bounced back and forth on the mirrors, land on their own photodiode. Therefore, any interruption of the "planes"

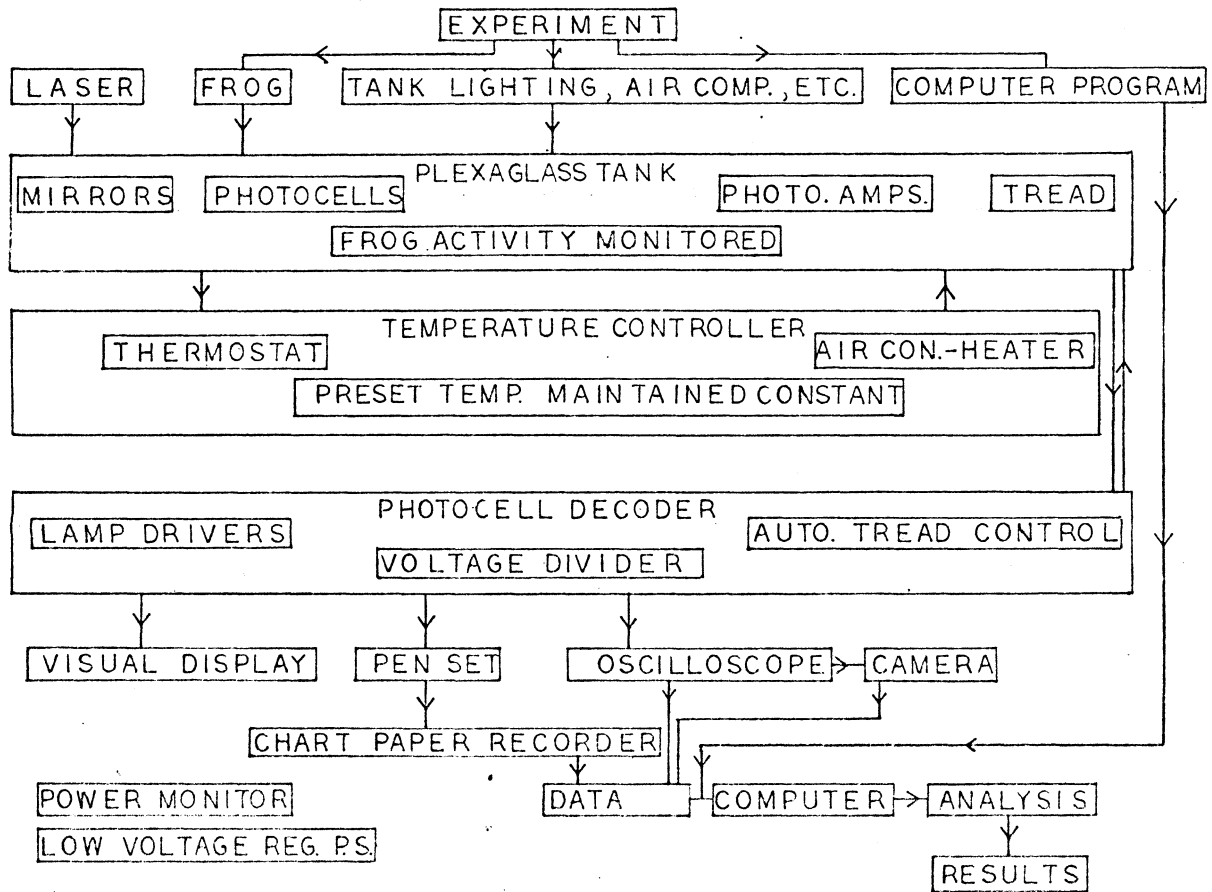


Fig. 3. The Laser Activated Amphibian Monitor System (LAAMS). Work development in the muscles of the jumping frog (or toad) can be measured automatically while the environment in which the frog is jumping can be controlled with regards to temperature, noise levels, lighting, humidity, and air composition. The laser used in the system is the Bausch and Lomb Helium-Neon Gas Laser. (.1 mm multimode). (Safety precautions necessary when using lasers in the laboratory can be found in the Handbook of Laboratory Safety, CRC 1967). Additional information on the system can be found in "LAAMS: Design, Circuit Theory and Construction Techniques" by Steven Saliterman, 1973.

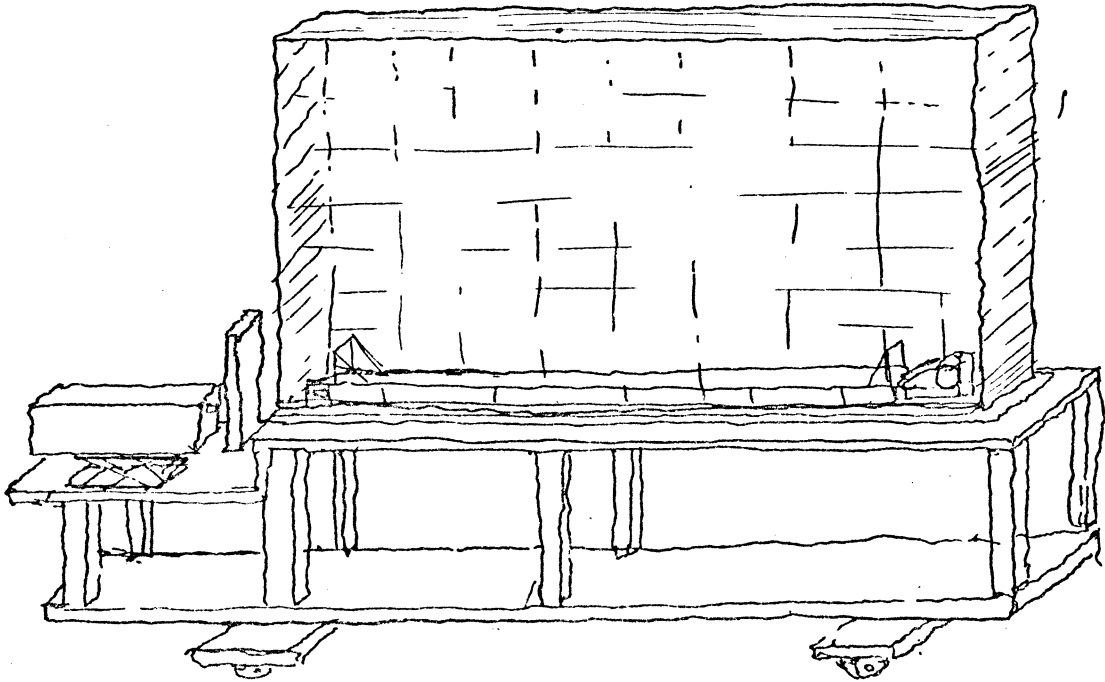


Fig. 4. Sketch of the tank used in LAAMS.

causes a corresponding loss of illumination of the corresponding photodiode. The lower photodiode is labeled DA, the upper photodiode DB. In addition to these two light receivers, a third photodiode (DC) is located at the "zero line" at tread level and is illuminated by a source shining perpendicular to the direction of tread travel. Table 1 shows the activity of the frog as it relates to the state of the individual light sensors.

<u>Activity</u>	<u>Photodiode</u>			<u>Photodecoder Voltage</u>
	<u>DA</u>	<u>DB</u>	<u>DC</u>	
at rest	off	on	off	1 volt
accelerating	off	off	on/off	3 volts
in flight	on	off/on	on	4 volts
decelerating	off	off	on	3 volts
being returned	off	on	on	2 volts

Table 1. eg. When the frog is accelerating, both planes are blocked and photodiodes A, B, and C are "off". The output voltage of the photodecoder is 3 volts. (explained later). When the frog first begins to accelerate its head rises and blocks beam DB. When acceleration ends and flight begins, DA is instantly turned on again. (DB may be either on or off during the flight phase). Deceleration begins and flight ends when the frog first touches the tread again. This is detected by DA suddenly going from on to off. Deceleration ends when the frog is at rest and DB is once again on. This position-rest away from the "zero line"-is detected by DC being on. The tread is automatically activated and the frog is brought back to the "zero line".

The three photodiodes signals enter (via amplifiers) a photocell decoder device. This device translates the binary type code word of the three photodiodes into four discrete output channels--each representing a given activity of the frog. (acceleration and deceleration activate the same channel). These channels (if desired) may each be connected to an individual electronic timer that will record the length of time each channel is "activated". The timers can then be connected via a memory unit to a teletype output device. The method currently being used is to voltage divide the 4 volt "activated" signal of each channel so that each channel produces a different voltage (see table 1). These outputs can then be tied together and fed into an oscilloscope and paper recorder.

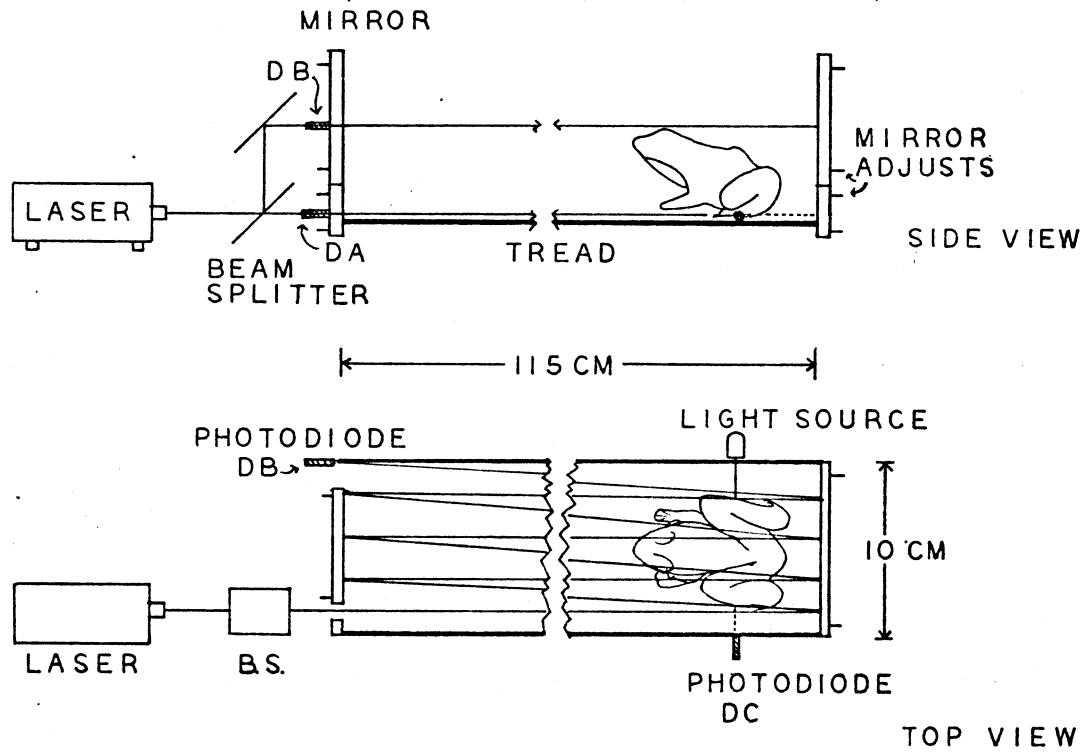


Fig. 5. Position of the upper and lower "planes" of laser light. The lower beam is blocked by the frog while the upper beam (positioned just above the head) is unobstructed. Photodiode DA is "off" while photodiode DB is "on". A third beam crosses the tread at the zero-line. When the frog is at rest at the zero-line photodiode DC is off. When the frog accelerates both DA and DB are off (DC is ignored). Flight is indicated when DA goes on (DB is ignored), and terminated when DA goes off. During deceleration both DA and DB are off. When the frog is again at rest DA is off while DB and DC are on. This combination causes the tread to automatically start. The tread stops when the frog is back at the zero-line and DC is off.

The output voltage will with time produce the graph seen in figure 6. The oscilloscope sweep rate is set so that it can record the acceleration time, flight time and deceleration time in a single sweep. The recorder measures the return time. Several scope traces can be recorded on a single picture by slightly advancing the horizontal adjust after each jump.

Test runs have shown that the frog can be made to jump by a mild current-limited electric shock. When external lights are off and the inside of the tank illuminated with a blue light, the frog will jump down the length of the tank without hitting the sides. The preference for blue light by frogs has been demonstrated by Muntz (19) and Torelle (20).

The data necessary for future calculations is obtained in the following way. Time of flight and acceleration are read off of the photographs from the oscilloscope camera. The return time is determined by the length of the trace on the paper recorder. This time is then multiplied by the tread's velocity so that B^1 is obtained. The tread is activated by a rapid start motor and little time is lost in coming to a uniform velocity.

$$B^1 = \text{Return Time} \times \text{Tread Velocity}$$

The frog may jump before being fully returned as well as jump so far that it hits the end wall. In either case data from that jump must be discarded and indication of the "bad" data should be made on the paper recorder. Experience has shown that the frog quickly learns to jump only when it must - and the electric shock appears to be sufficient reason to jump. The sudden starting of the tread does not seem to cause the frog to jump. Future experiments might consist of a series of ten shocks spaced a minute apart. The interval between shocks is arbitrary and is chosen so as to produce the most desirable work development decay curve. Once the interval is chosen it must be maintained throughout the experiment. If the interval is too long the frog may fully recover from the previous jump and no decay curve would be obtained. If the interval is too short the frog may quit responding to the mild shock.

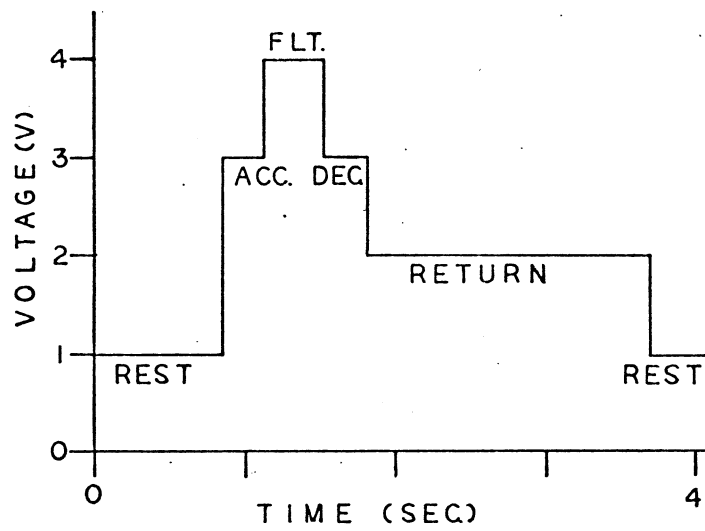


Fig. 6. Output voltage of the photodecoder. A different voltage corresponds with each activity of the frog. The signal above was selected so that the output would "somewhat" resemble a jump!

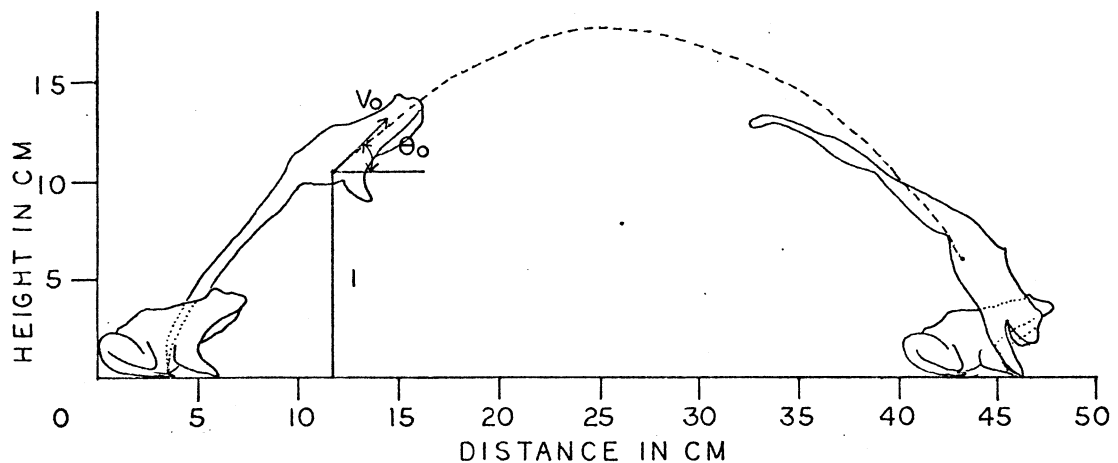


Fig. 7. Stages of the frog's jump and pathway taken by the center of mass during flight. Notice that the center of mass during flight travels further coming down from the summit of the trajectory than going up to the summit.

Mathematical Analysis of Frog Jumping

The following definitions correspond with the points and segments of figures 8 and 9:

- P1 Hind end of frog before jump
 P2 Tips of toes before jump
 P3 Center of mass before jump
 P4 Center of mass at instant of take off
 P5 Intersection with x axis of vertical segment from P4
 P6 Tips of fingers before jump
 P7 Intersection with path of c.d.m. of a horizontal segment from P4
 P8 Intersection of a vertical segment through P7 with a horizontal through P9
 P9 Center of mass at instant of landing
 P10 Intersection with x axis of a vertical segment from P9
 P11 Tips of fingers after landing
 P12 Hind end of frog after landing
 P13 Center of mass after landing
 P14 Tips of toes after landing
 P15 Intersection with x axis of a vertical segment from P3
 P16 1/2 the distance from P4 to P7
 P17 Highest point reached by the center of mass (summit)

- A P2-P11 $A=B+D$
 B¹ P1-P12 Measured by LAAMS
 B P6-P11 $B=B^1$
 C P5-P10 $C=A-O-N$
 D P2-P6 Measured before jump
 E P4-P7 $E=(V_o^2 \sin(2\theta))/g$
 F P3-P4 discussed later
 G P2-P3 discussed later
 H P2-P4 Measured before jump
 I P5-P4 $I=H\sin\theta_o$
 J P7-P8 $J=-(t_f V_o \sin\theta_o - .5gt_f^2)$
 K P8-P9 $K=t_f V_o \cos\theta_o - (2V_o^2 \sin\theta_o \cos\theta_o)/g$

L	P9-P10	$L = M \sin \theta_o$
M	P9-P11	Measured before jump
N	P10-P11	$N = M \cos \theta_w$
O	P2-P5	$O = H \cos \theta_o$
Q	P3-P15	Measured before jump
S	P16-P17	$S = (V_o^2 \sin^2(\theta_o)) / (2g)$

V_o initial velocity

V_w reentry velocity $V_w = ((V_o \cos \theta_o)^2 + (V_o \sin \theta_o - g t_f)^2)^{1/2}$

θ_o angle of initial velocity vector

θ_w reentry angle $\theta_w = \tan^{-1}((V_o \sin \theta_o - g t_f) / (V_o \cos \theta_o))$

t_f time of flight - measured by LAAMS

t_a time of acceleration - measured by LAAMS

Segments E, J, K and S, and V_w and θ_w are determined in the following way:

1.) The x and y components of V_o are

$$V_{ox} = V_o \cos \theta_o \quad V_{oy} = V_o \sin \theta_o$$

The components of V are

$$V_x = V_o \cos \theta_o \quad V_y = V_o \sin \theta_o - g t$$

The magnitude of the resulting vector at any instant is

$$V = (V_x^2 + V_y^2)^{1/2}$$

The angle θ makes with the horizontal at that instant is

$$\theta = \tan^{-1}(V_y / V_x)$$

2.) The x-coordinate of the center of mass at any time is

$$x = (V_o \cos \theta_o) t$$

The y-coordinate is

$$y = (V_o \sin \theta_o) t - .5 g t^2$$

3.) The general equation for the parabolic trajectory is

$$y = (\tan \theta_o) x - g / (2 V_o \cos \theta_o)^2$$

4.) $\theta_w = \tan^{-1}((V_o \sin \theta_o - g t_f) / (V_o \cos \theta_o))$

$$V_w = ((V_o \cos \theta_o)^2 + (V_o \sin \theta_o - g t_f)^2)^{1/2}$$

5.) t_f = time of travel of center of mass from P4 to P9

Let t_e = time of travel of center of mass from P4 to P7

If an additional equal coordinate system is applied to figure 9 with origin at P4, then the y' -coordinate at P7 must equal zero.

$$y' = 0 = (V_o \sin \theta_o) t_e - .5gt_e^2$$

$$\text{Therefore } t_e = (2V_o \sin \theta_o / g)$$

6.) $E = t_e V_o \cos \theta_o = V_o^2 \sin(2\theta_o) / g$

7.) Let t_s = time center of mass takes to travel from P4 to P17

$$V_o \sin \theta_o = gt_s$$

$$t_s = (V_o \sin \theta_o) / g$$

$$\text{Let } P17 = (x'_{17}, y'_{17})$$

$$x'_{17} = E/2 = V_o^2 \sin(2\theta_o) / (2g)$$

$$y'_{17} = t_s V_o \sin \theta_o - (gt_s^2) / 2 = V_o^2 \sin^2 \theta_o / (2g)$$

$$\text{Therefore } s = (V_o^2 \sin^2 \theta_o) / (2g)$$

8.) $P7 = (x'_7, y'_7) = ((2V_o \sin \theta_o / g) (V_o \cos \theta_o), 0)$

$$P9 = (x'_9, y'_9) = (t_f V_o \cos \theta_o, t_f V_o \sin \theta_o - .5gt_f^2)$$

$$K = (x'_9 - x'_7) = t_f V_o \cos \theta_o - (2V_o^2 \sin \theta_o \cos \theta_o) / g$$

$$J = (y'_9 - y'_7) = t_f V_o \sin \theta_o - .5gt_f^2$$

Segments H, M, and Q are determined by a simple center of mass exercise performed with each frog. Figures 10 and 11 show the general procedure used for locating the center of mass. An anesthetized frog is tied together with light thread so that its limbs are in a position resembling that of rest. Two photographs are taken - each picture being of the frog suspended from a different point along the plane of symmetry. The photographs are then superimposed and the center of mass estimated by the intersection of the projected suspension lines. The distance from the center of mass to the usual ground is Q. The distance from the tips of the toes to the tips of the fingers in the resting frog is easily measured while the frog is in the tank waiting to jump. Two determinations are made on the stretched frog.

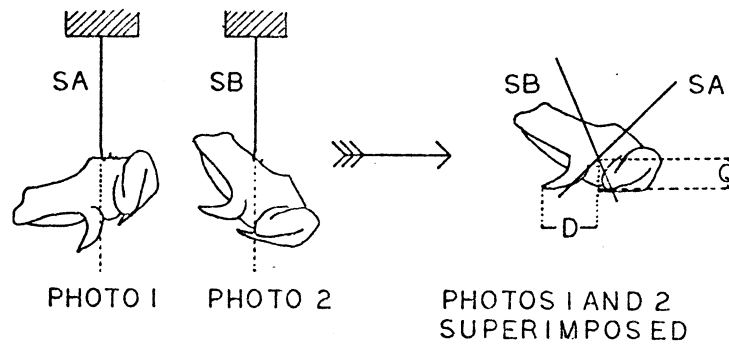


Fig. 10. Determination of center of mass in the "resting frog" (see text for procedure).

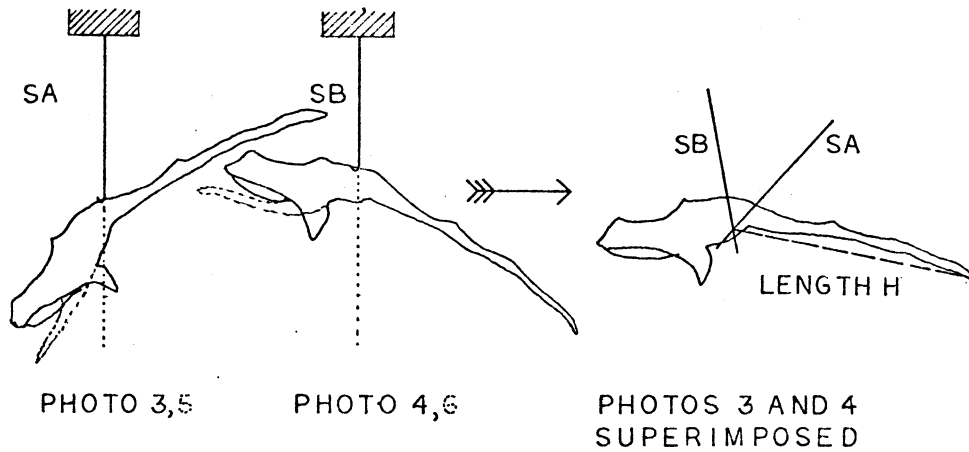


Fig. 11. Determination of center of mass in the "stretched" frog. Two determinations are made—one with the fore limbs back for measurement of H, the other with the fore limbs forward for measurement of M.

The first is done with the fore limbs tied back. This allows for measurement of H, the distance from the tips of the toes to the center of mass. The second determination is done with the fore limbs tied forward. This allows for determination of M, the distance from the tips of the fingers to the center of mass. In both determinations it is helpful to tie the frog to a thin rod placed down the length of the frog on its back. The suspension line is fastened to the center of the rod. The frog is then moved up or down the rod so that two pictures of different orientation can be taken.

At this point we can summarize the nine known variables.

M, H, and Q - determined by center of mass exercise

D - measured while the frog is resting in the tank

B^1, t_f, t_a - determined by LAAMS

M_f, M_m - mass of the frog and of the muscles involved in jumping (obtained by dissection)

The remaining segments of figure 9, as well as V_w and θ_w have been given as functions of these variables and V_o and θ_o . The next step is show that V_o and θ_o are functions of the first six known variables above.

The following steps lead to three equations with three unknowns. The three unknowns are V_o , θ_o , and θ_w . When all angles are kept between 1° and 89° inclusive, there is only one solution set.

1.) As before

$$\theta_w = \tan^{-1}((V_o \sin \theta_o - gt_f) / (V_o \cos \theta_o)) \quad I$$

2.) From figure 9

$$J = I - L$$

$$B = A - D = B^1$$

$$A = C + O + N$$

$$C = K + E$$

3.) Therefore

$$B^1 = A - D = C + O + N - D = K + E + O + N - D$$

$$B^1 = (t_f V_o + H) \cos \theta_o + M \cos \theta_o - D \quad II$$

4.) As before

$$J = -(t_f V_o \sin \theta_o - .5gt_f^2)$$

Therefore

$$J = I - L = H \sin \theta_o - M \sin \theta_w = -(t_f V_o \sin \theta_o - .5gt_f^2)$$

Solving for M

$$M = (H \sin \theta_o + t_f V_o \sin \theta_o - .5gt_f^2) / \sin \theta_w \quad \text{III}$$

In all of the equations g is 980 cm/sec^2 . The computer finds the solution set to equations I, II and III by means of a simple routine. θ_o is incremented 1° at a time. For each θ_o , V_o is incremented 1 cm/sec . The limits over which θ_o and V_o are incremented are determined by solving for approximate values for θ_o and V_o . The limits are set plus and minus some interval on either side of the approximate values. For each set of θ_o and V_o , the computer solves the right hand sides of equations II and III and compares the answers to the known left hand sides. The computer then selects the best solution set.

Little has been said so far about the pathway taken by the center of mass during acceleration and deceleration. As we have already seen this information is not necessary for calculation of V_o and θ_o . The curved path taken during acceleration can be visualized by inspecting Hirsch's drawings (figures 1 and 2). During deceleration the center of mass continues forward for a few moments and then drops down and backward. P13 is not involved in any of our calculations.

A very rough approximation of the initial velocity could be obtained by assuming uniform acceleration over the segment F. F is calculated from H, G and the angle P3-P2-P15. \bar{V}_o is then equal to $2F/t_a$. This equation is not used in any form in this project.

Obtaining Work Development

The computer program listed here is capable of handling the data from twenty frogs making ten jumps each (smaller numbers may be used). The data from four frogs making two jumps each has been simulated and entered into the program (see data at end of computer program). Frog 1 has been labeled "control." Thirty variables are listed and under each the appropriate value for the particular jump. The nine known values entered into the program as data are circled. The remaining

variables are solved by the formulas already described and by the following:

$$\text{Potential Energy} = \text{PE} = M_f g (I-Q)$$

$$\text{Kinetic Energy} = \text{KE} = .5 M_f V_o^2$$

$$\text{Work Development} = (\text{KE} + \text{PE}) / t_a * M_m$$

$$\text{Power Development} = 5(\text{Work Development})$$

(where efficiency of the muscle has been arbitrarily set at 20%)

$$\text{Approximate } V_o = (B^1)^2 / t_f^2 + (t_f^2 g^2 / 4)$$

$$\text{Approximate } \theta_o = \sin^{-1} (t_f g) / (2 V_o)$$

These approximate values are used only to define a region of V_o and θ_o that the computer can use to rapidly find the real V_o and θ_o . The values in the output labeled F1 and F2 are the final solutions to equations II and III reached by the computer. These values agree fairly well with the actual B^1 and M , and indicate that V_o is known to the nearest cm/sec and θ_o is known to the nearest degree. (this has been varified by letting the computer print out an entire family of solns. as V_o and θ_o are incremented)

In summary, inserting the nine circled variables allows for determination of work development. The other values determined are just nice things to have around. The next step in an experiment would be to graph work development against jump number for each frog. The control group data would then be statistically compared to the experimental group in hopes of finding significant differences.

A Final Note on Air Resistance

Up to now we have neglected air resistance and made our calculations as if the frog were in a vacuum. As we will soon see the effect of drag has almost no consequences on the determination of V_o and θ_o . Equations I,II,III described earlier may be modified to conform with the additional force of drag, F_d .

$$\text{I. } \theta_w = \tan^{-1} ((V_o \sin \theta_o - (\sin \theta / M_f) \int_{t=0}^{t_f} F_d dt - t_f g) / (V_o \cos \theta_o - (\cos \theta / M_f) \int_{t=0}^{t_f} F_d dt))$$

$$\text{II. } B^1 = (t_f V_o \cos \theta_o - ((.5 \cos \theta_o / M_f) \int_{t=0}^{t_f} t^2 F_d dt)) + H \cos \theta_o + M \cos \theta_w - D$$

$$\text{III. } M = (H \sin \theta_o + t_f V_o \sin \theta_o - (.5 \sin \theta_o / M_f) \int_{t=0}^{t_f} t^2 F_d dt) / \sin \theta_w$$

The problem now becomes one of solving the two integrals used above.

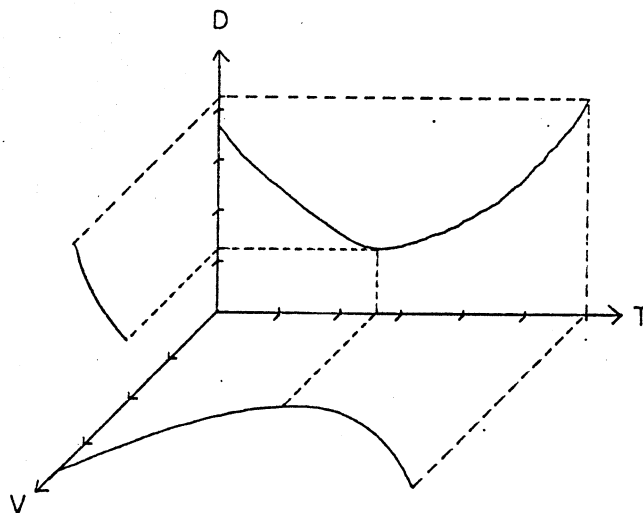


Fig. 12. General relationship between drag, velocity and time for a frog in flight.

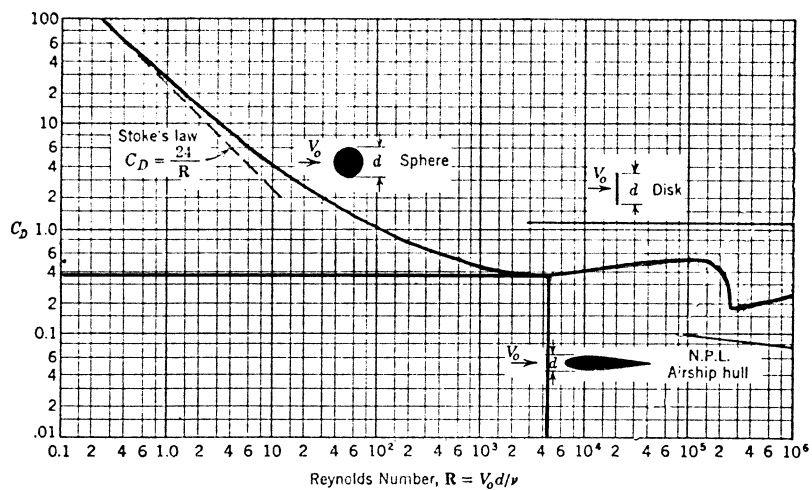


Fig. 13. Reynolds number and coefficient of drag for a sphere, airship hull and disk. A sphere of diameter 4 cm. is used in the sample calculation. It should be realized that a frog in flight is more streamlined and suffers less drag than does the sphere of similar dimensions.

The general relationship between drag, time, and velocity of a jumping frog is shown in figure 12. The maximum drag occurs when the frog is traveling with its greatest velocity. The maximum velocity occurs at a time t_f -- when the frog has a final reentry velocity greater than its initial velocity V_0 . The relationship between drag and time is arrived at by first determining the relationship between drag and velocity over the velocities concerned. This information along with the relationship between time and velocity allows the drag as a function of time to be determined. Once the drag as a function of time is known the integrals described above are easily solved.

For a sample calculation of the drag function we will use the simulation data of frog 1 in the computer output. The important data are $V_w = V_{\text{maximum}} = 189^\circ$, $V_{\text{minimum}} = V_0 \cos \theta_0 = 109 \text{ cm/sec}$, $V_0 = 177 \text{ cm/sec}$ and $\theta_0 = 52^\circ$. Other necessary data include the viscosity, kinematic viscosity and density of dry air at 18 degrees centigrade at 1 atmosphere.

$$\begin{aligned} \text{viscosity} &= \mu = 182.7 \times 10^{-6} \text{ g/sec-cm} \\ \text{kinematic viscosity} &= \nu = 1.54 \times 10^{-1} \text{ cm}^2/\text{sec} \\ \text{density} &= \rho = 1.2 \times 10^{-3} \text{ g/cm}^3 \end{aligned}$$

Using the Reynold number vs. coefficient of drag chart (fig. 13) table 2 can be constructed (21). The frog is imagined as a sphere with diameter $d=4\text{cm}$. "A" in table 2 is equal to $\pi(d/2)^2$.

V	$R=(V d/\nu)$	C_d	$F_d = (C_d \rho V^2 A) / 2$
177	4600	.4	380 g-cm/sec ²
180	4680	.4	392
183	4750	.4	406
186	4830	.4	418
189	4900	.4	431

Table 2. Calculation of drag for various velocities from V_{maximum} to V_{minimum} for frog 1. These results are graphed in figure 14.

Velocity is related to time by $v = (V_0 \cos \theta_0)^2 + (V_0 \sin \theta_0 - gt)^2)^{1/2}$. The simulation data of frog 1 gives a time of flight $t_f = .3 \text{ sec}$. Intervals of .05 sec are graphed against the resulting velocity in figure 15. Table 3 gives the values used.

t =	0	.05	.1	.15	.2	.25	.3
v =	177	140	115	109	121	151	189

Table 3. Relationship between velocity and time, from simulation data of

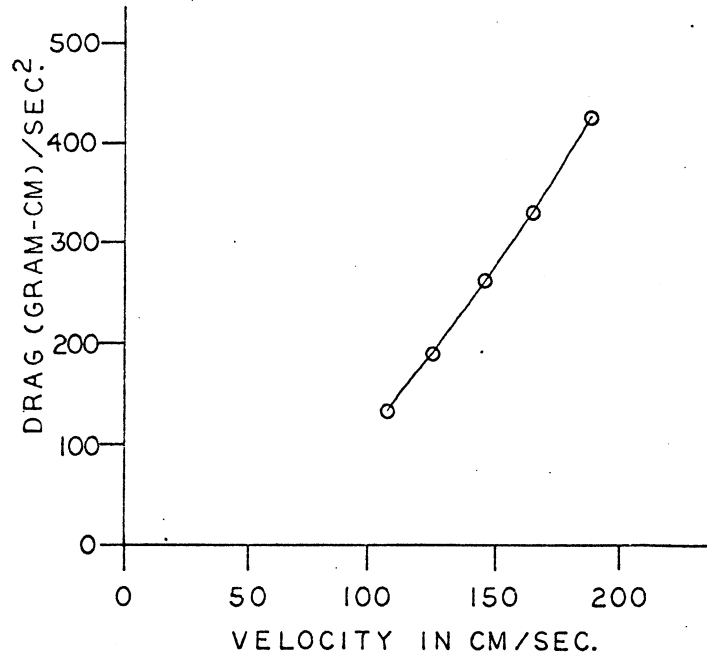


Fig. 14. Drag plotted against velocity.

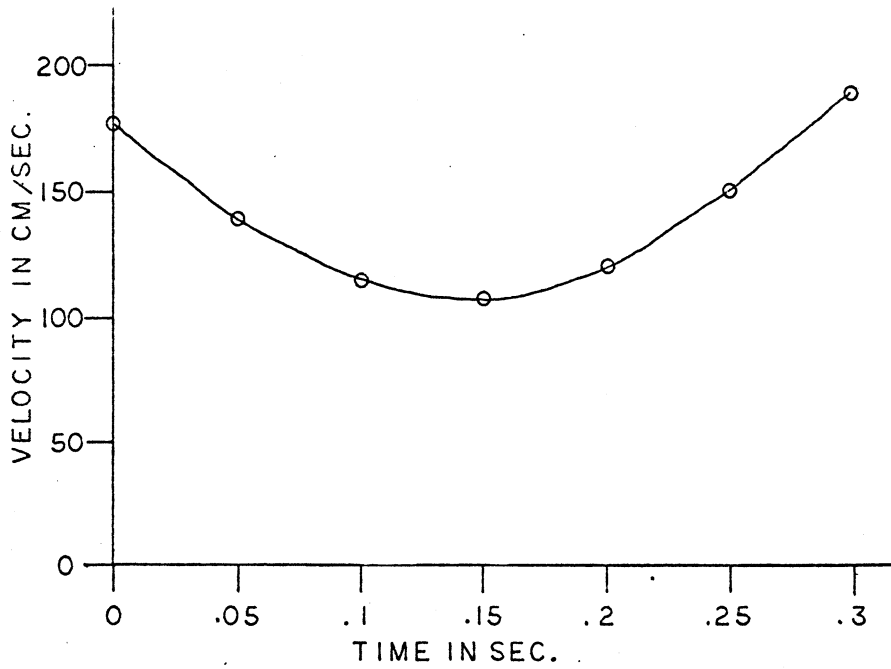


Fig. 15. Velocity plotted against time.

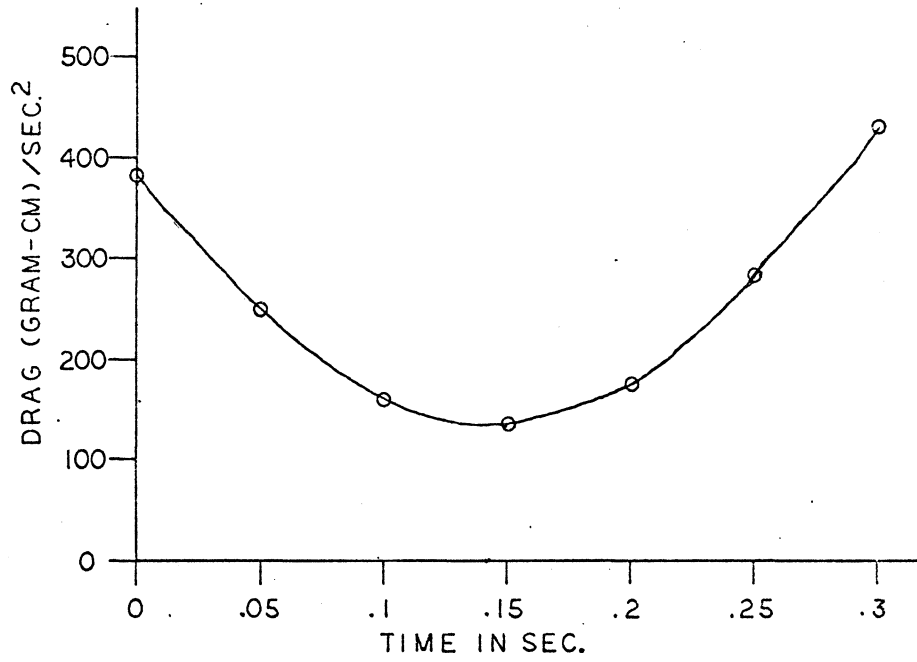


Fig. 16. Drag plotted against time.

frog 1.

It is now possible to find the relationship between drag and time. Because the coefficient of drag, C_d , is constant over the velocities involved, F_d is proportional to V^2 . Inspection of table 2 shows that $F_d = 1.21 \times 10^{-2} V^2$. Replacing V by $((V_0 \cos \theta_0)^2 + (V_0 \sin \theta_0 - gt)^2)^{1/2}$ gives the following function for F_d :

$$F_d = 3.69 \times 10^2 - 3.32 \times 10^3 t + 1.16 \times 10^4 t^2 = a - bt + ct^2 \quad \text{and} \quad \int_{t=0}^{t_f} F_d dt = \frac{at_f^2}{2} - \frac{bt_f^3}{3} + \frac{ct_f^4}{4} \quad \text{and} \quad \int_{t=0}^{t_f} t^2 F_d dt = \frac{at_f^3}{3} - \frac{bt_f^4}{4} + \frac{ct_f^5}{5}$$

The insertion of these integrals into the modified equations described at the beginning of this section do not significantly alter the final determination of V_0 and θ_0 . Using the values for a, b and c in the example above does not result in a new V_0 and θ_0 when V_0 is measure to the nearest cm/sec and θ_0 measured to the nearest degree. Drag vs. time for the above example is graphed in figure 16. Rapid inspection shows that for a 100g frog the max. acceleration experienced opposite to the direction of motion is about 4 cm/sec². This has a small influence when compared to the 980 cm/sec² downward acceleration due to gravity. Strictly speaking however, the drag causes a path of travel of the center of mass that is not exactly a parabola.

The values used for a, b and c in the above example were derived by using the V_0 as if in a vacuum. This allowed the two integrals and a new V_0 and θ_0 to be calculated. In reality we have only found the first approximation to the real V_0 and θ_0 . The next step would be use the new V_0 and θ_0 to calculate a better set of values for a, b and c . The actual values for V_0 and θ_0 would be arrived at by successive approximation. Fortunately, not even the first calculation is necessary for this experiment!

Program Operating Structure

The following information includes all the necessary information for running the program on the CDC 3300.

```
$JOB, ID, NAME, 2,2000
$SCHED, CORE=60, SCR=3, CLASS=C
$FTN (L,X,M)
(Program)
END (column 7)
```

FINIS (column 10)

\$ X, LGO

(DATA)

~~77~~
88

Data is in the following format

Card 1 Any alphanumeric comment columns 2-80

Card 2 Any alphanumeric comment columns 2-80

Card 3 Total number of frogs. Two digit integer value in columns 1 and 2. (must be 20 or less).

Card 4 Frog characteristic card

Variable	Starting Column	Format
Frog I.D.	1	I3
Control/Exper.	6	A8
Number of jumps	16	N2 (max. no. is 10)
Mass of frog (g)	20	F 6.2
H (cm)	28	F 5.2
M (cm)	35	F 5.2
D (cm)	42	F 4.2
Mass of muscle (g)	48	F 6.2
Q	56	F 4.2

Card 5 Jump Data for first jump.

Time of flight (sec.)	5	F 4.2
Time of acceleration (sec)	11	F 4.2
B' (cm)	17	F 6.2

Card 6-n Remainder of jump data for frog identified in card 4. The jump data cards are arranged in the same order as the jumps were made. One card is used for each jump.

Card n+1-last card

Repeat as in card 4 for next frog. Place jump data immediately after frog characteristic card. Follow this procedure until all frogs and all jumps are included.

Design of the Computer Program

The following letters and descriptions refer to sectioned blocks labeled on the computer program.

- A. Storage allocation of arrays
- B. Input and output of data cards one and two.
- C. Input of total number of frogs
- D. Input of characteristics of an individual frog.
Identification number, control/experi., total number of jumps by this frog, mass of the frog, M , D , mass of the muscles, Q .
- E. Input of jump data
Time of flight, time of acceleration, B
- F. Acceptance range used later in comparing F_1 and F_2 to the real B and M .
- G. This loop increments frog being analyzed
- H. This loop increments jump number of particular frog being analyzed
- I. Used as counter
- J. Assignment of array variables to "easier to handle" variables.
- K. Determination of an approximate V_0 and approximate θ_0 used to determine the limits over which a search for the actual V_0 and θ_0 will be conducted.
- L. Loop increments θ_0 being tested in equations I,II, and III.
- M. Loop increments V_0 being tested in equations I,II, and III.
- N. Equation I.
- O. Equation II.
- P. Equation III.
- Q. If a soln. to equations I,II and III is reached with the accuracy set by (F) above, this block is reached. The V_0 , θ_0 , θ_w , F_1 and F_2 that are currently being used are stored for later evaluation. The computer then returns and searches for more possible solutions.
- R. After all possible solutions have been reached, the computer here selects the solution in which the sum of the absolute errors of F_1 to B and F_2 to M is smallest. Once the solution has been obtained, the correct V_0 , θ_0 , θ_w and final F_1 and F_2 are save for use in (S).
- S. Calculation of other dimensions associated with the jump, and storage in "w" arrays. These "w" arrays are eventually printed out.

w1= V_0	w7=PE	ww1= F_1	ww7=L	ww13=K
w2= θ_0	w8=KE	ww2= F_2	ww8=I	ww14=S
w3= V_w	w9=WD	ww3=B	ww9=J	ww15=AVO
w4= θ_w	w10=PP	ww4=M	ww10=A	ww16=CATO
w5=Q	w11= M_f	ww5= T_f	ww11=E	
w6=I+S	w12=Mm	ww6= T_a	ww12=C	

- T. Return to next jump or to next frog
- U. Print out of calculations

References

1. Mountcastle, Vernon B. Editor. Medical Physiology. Saint Louis: C.V. Mosby Company (1968) II, pp. 1128-1171.
2. Hill, A. V. (1938) Proc. Roy. Soc. Lon. B, 126, pp. 136-195.
3. Hill, A. V. (1956) Brit. M. Bull, 12, pp. 174-176.
4. Hill, A. V. First and Last Experiments in Muscle Mechanics. Cambridge: University Press (1970).
5. Mountcastle II, pp. 1144-1147.
6. Carlson, Francis D., Hardy, Donna J., and Wilkie, Douglas R. (1963) J. Gen. Physiol., 46, pp. 851-8821.
7. Huxley, H.E. (1969) Science, 164, pp. 1356-1366.
8. Maruyama, Koscak, and Weber, Annemarie. (1972) Biochemistry, 11, 16, pp. 2990-2997.
9. Rand, Stanley A. and Rand, Patricia J. (1966) Herpetologica, 22, 3, pp. 207-208.
10. Rand, Stanley A. (1952) Copeia, 1, pp. 15-21.
11. Stokely, P.S. and Berberian, J.F. (1953) Copeia, e, p. 187.
12. Gans, Carl and Rosenberg, H.J. (1966). Herpetologica, 22, 3, pp. 209-213.
13. Gans, Carl and Parsons, Thomas S. (1965) Evolution, 20, 92-99.
14. Gray, James. Animal Locomotion.
15. Gray, James. How Animals Move. Cambridge: University Press (1953).
16. Hirsch, Walter. (1931) Zeitschrift Fur Vergleichende Physiologie, 15, 1931, pp. 1-49.
17. Zug, George R. (1972) Copeia, 4, pp. 613-624.
18. Mountcastle II, p. 1141.
19. Muntz, W.R.A. (1964) Scientific American, 210, pp. 110-119.
20. Torelle, Ellen. (1903) American Journal of Physiology, 9, pp. 466-488.
21. Vennard, John K. Elementary Fluid Mechanics. New York: John Wiley and Sons, Inc., (1961).

Acknowledgements

I wish to thank the many individuals and companies who have "leaped" far beyond the call of duty in assisting me with this project.

Mr. William Anderson

Dr. H. Mead Cavert

Mr. Michael Coscio

Mr. Bruce Eaton

Mr. Elmer Frykman

Mr. Merle Hillman

Dr. Frank D. Hirschback

Dr. Warren E. Ibele

Mr. Bob Isenberg

Mr. Eric Johnson

Dr. John A. Johnson

Dr. Walter H. Johnson

Dr. Richard McGehee

Mr. Jim McGinnis

Pat Percy

Mr. Richard C. Peterson

Mr. Dale Reedstrom

Mr. Bob Ritter

Mr. Larry Roberts

Dr. Robert L. Sorenson

Mr. Richard Stish

Mr. Jim Weins

Dr. Donald B. Wetlaufer

Allied Plastics

Baush and Lomb

Curtin Matheson Scientific

General Electric

Honeywell

Magnetic Controls

Texas Instruments

Moreover, I am equally grateful to the many other individuals who have patiently listened to my ideas and who have given suggestions that have improved the course of the project. Many topics explored with these individuals are still in the "works" and will be presented at a later date.

Additional invaluable assistance has been obtained from the University of Minnesota Honors Department and the Health Computer Science Center.

I especially would like to thank my advisors, Dr. John A. Johnson and Dr. H. Mead Cavert for the encouragement they have given me during the past three years.

JOB ACCOUNTING INFORMATION

NAME=SSS ACCT=GRAD29

DATE=06/18/73 EDITION=3M TIME-ON=17/58/59 TIME-OFF=18/00/30

TIME USED

COMP=00/01/17.382

CHAN=00/00/02.749

TERMINAL=00/00/00.000

FACILITIES NOT USED

CORE=006

SCR =000

LINE=1691

CARD=0

SUM OF OUT+PLT BLOCKS= 15

JOB,GRAD29,SSS,2,2000
SCHED,CORE=60,SCR=3,CLASS=C
FTN(L,X,M)

PROGRAM FROGJUMP

```

DIMENSION SC1(20),SC2(20),NSID(20),SGG(20),SMASS(20),SH(20),SM(20),
1,SD(20),NSTNJ(20),SMASSM(20),STF(20,10),STA(20,10),SG(20,10)
1,SF1(20),SF2(20),
1W1(20,10),W2(20,10),W3(20,10),W4(20,10),W5(20,10),W6(20,10),
1W7(20,10),W8(20,10),W9(20,10),W10(20,10),W11(20,10),W12(20,10)
1,WW1(20,10),WW2(20,10),WW3(20,10),WW4(20,10),WW5(20,10),
1WW6(20,10),WW7(20,10),WW8(20,10),WW9(20,10),WW10(20,10),
1WW11(20,10),WW12(20,10),WW13(20,10),WW14(20,10),WW15(20,10),
1WW16(20,10),WWW1(20,10),WWW2(20,10),SF3(20),SF4(20)
1,TT(20)
1,SB(20,10)
1,WWW3(20,10),WWW4(20,10),SF5(20),SF6(20)
1,SQ(20)

```

A

INTEGER TNF

```

READ(60,1)(SC1(KA),KA=1,10)
READ(60,1)(SC2(KB),KB=1,10)
1 FORMAT(10A8)
WRITE(61,3)(SC1(KC),KC=1,10)
WRITE(61,3)(SC2(KD),KD=1,10)

```

B

```

3 FORMAT(//10A8)
READ(60,33)TNF
33 FORMAT(I2)

```

C

```

DO 5 KE=1,TNF
READ(60,44)NSID(KE),SGG(KE),NSTNJ(KE),SMASS(KE),SH(KE),SM(KE),
1SD(KE),SMASSM(KE),SQ(KE)
44 FORMAT(I3,2X,A8,2X,I2,2X,F6.2,2X,F5.2,2X,F5.2,2X,F4.2,2X,F6.2
1,2X,F4.2)

```

D

```

INJ6=NSTNJ(KE)
DO 5 KF=1,INJ6
READ(60,6)STF(KE,KF),STA(KE,KF),SB(KE,KF)
5 CONTINUE

```

E

```

6 FORMAT(4X,F4.2,2X,F4.2,2X,F6.2)
G=980
CC1=.5
CC2=.5

```

F

```

DO 29 JF=1,TNF
INJ5=NSTNJ(JF)

```

G

```

DO 29 JJ=1,INJ5
K=0

```

H

```

TF=STF(JF,JJ)
B=SB(JF,JJ)
H=SH(JF)
ZM=SM(JF)

```

I

```

ZMF=SMASS(JF)
ZMM=SMASSM(JF)
D=SD(JF)

```

J

```

AVO=((TF**2*G**2)/4+B**2/TF**2)**.5
XX=(TF*G)/(2*AVO)
ATO=ATAN(XX/((1-(XX)**2)**.5))
Q1=AVO+25
Q=AVO-100
IF(Q.LE.0)Q=1
CATO=ATO*360/(2*3.14)

```

K

```

      Q4=CAT0+15
      Q3=CAT0-15
      IF(Q3.LE.0)Q3=1
      IF(Q4.GE.90)Q4=89
      INJ1=Q
      INJ2=Q1
      INJ3=Q3
      INJ4=Q4
      DO 10 J=INJ3,INJ4
      XJ=J
      T0=(XJ*3.14*2.0)/360.0
      DO 10 IVO=INJ1,INJ2
      V0=IVO
      TW=ATAN(ABS((V0*SIN(T0)-G*TF)/(V0*COS(T0))))
      F1=(TF*V0+H)*COS(T0)+ZM*COS(TW)-D
      IF(ABS(B-F1).LE.CC1)7,9
      F2=(H*SIN(T0)+TF*V0*SIN(T0)-.5*G*TF*TF)/SIN(TW)
      IF(ABS(ZM-F2).LE.CC2)8,9
      K=K+1
      TT(K)=(ABS(B-F1))/B+(ABS(ZM-F2))/ZM
      SF1(K)=F1
      SF2(K)=F2
      SF3(K)=V0
      SF4(K)=XJ
      SF5(K)=TW
      SF6(K)=T0
      CONTINUE
      DO 11 IY=1,K
      DO 101 JY=1,K
      IF(TT(IY).LE.TT(JY))GO TO 101
      GO TO 11
      CONTINUE
      WW1(JF,JJ)=SF1(IY)
      WW2(JF,JJ)=SF2(IY)
      WWW1(JF,JJ)=SF3(IY)
      WWW2(JF,JJ)=SF4(IY)
      WWW3(JF,JJ)=SF5(IY)
      WWW4(JF,JJ)=SF6(IY)
      GO TO 12
      V0=WWW1(JF,JJ)
      XJ=WWW2(JF,JJ)
      TW=WWW3(JF,JJ)
      T0=WWW4(JF,JJ)
      W1(JF,JJ)=V0
      W2(JF,JJ)=XJ
      W3(JF,JJ)=((V0*COS(T0))**2+(V0*SIN(T0)-G*TF)**2)**.5
      W4(JF,JJ)=TW*360/(2*3.14)
      W5(JF,JJ)=SQ(JF)
      W6(JF,JJ)=H*SIN(T0)+((V0**2)*SIN(T0)**2)/(2*G)
      W7(JF,JJ)=ZMF*G*(H*SIN(T0)-SQ(JF))
      W8(JF,JJ)=.5*ZMF*V0**2
      W9(JF,JJ)=(W7(JF,JJ)+W8(JF,JJ))/((ZMM)*STA(JF,JJ))

```

K

L

M

N

O

P

Q

R

S

7

8

9

10

101

11

12

W11 (JF, JJ) = ZMF
W12 (JF, JJ) = ZMM

WW3 (JF, JJ) = B
WW4 (JF, JJ) = ZM
WW5 (JF, JJ) = TF

WW6 (JF, JJ) = STA (JF, JJ)
WW7 (JF, JJ) = ZM * SIN (TW)
WW8 (JF, JJ) = H * SIN (TO)

S

WW9 (JF, JJ) = WW8 (JF, JJ) - WW7 (JF, JJ)
WW10 (JF, JJ) = B + D
WW11 (JF, JJ) = V0 ** 2 * SIN (2 * TO) / G
WW12 (JF, JJ) = B + D - H * COS (TO) - ZM * COS (TW)
WW13 (JF, JJ) = WW12 (JF, JJ) - WW11 (JF, JJ)
WW14 (JF, JJ) = (V0 ** 2 * SIN (TO) ** 2) / (2 * G)

WW15 (JF, JJ) = AVO
WW16 (JF, JJ) = CATO

29 CONTINUE

T

DO 15 N1=1, TNF
WRITE (61, 80) NSID (N1), SGG (N1)
WRITE (61, 81)

13 INJ = NSTNJ (N1)
DO 13 N2=1, INJ
WRITE (61, 82) N2, W1 (N1, N2), W2 (N1, N2), W3 (N1, N2), W4 (N1, N2), W5 (N1, N2),
1 W6 (N1, N2), W7 (N1, N2), W8 (N1, N2), W9 (N1, N2), W10 (N1, N2), W11 (N1, N2),
1 W12 (N1, N2), SD (N1)
WRITE (61, 83)

14 DO 14 N3=1, INJ
WRITE (61, 84) N3, WW1 (N1, N3), WW2 (N1, N3), WW3 (N1, N3), WW4 (N1, N3),
1 WW5 (N1, N3), WW6 (N1, N3), WW7 (N1, N3),
1 WW8 (N1, N3), WW9 (N1, N3), WW10 (N1, N3), WW11 (N1, N3), WW12 (N1, N3),
1 WW13 (N1, N3), WW14 (N1, N3), WW15 (N1, N3), WW16 (N1, N3), SH (N1)

U

15 CONTINUE

80 FORMAT (///54X, 4HFROG, 2X, I3, 5X, A8)

81 FORMAT (//2X, 4HJUMP, 4X, 2HV0, 7X, 2HT0, 7X, 2HVW, 7X, 2HTW,
17X, 1HQ, 7X, 3HI+S

82 FORMAT (/3X, I2, 6(3X, F6.2), 4(3X, E8.2), 3(3X, F6.2))

83 FORMAT (///2X, 4HJUMP, 3X, 1HB, 7X, 1HM, 6X, 1HB, 7X, 1HM, 7X, 2HTF, 4X, 2HTA,
15X, 1HL, 6X, 1HI, 6X, 1HJ, 6X, 1HA, 6X, 1HE, 6X, 1HC, 6X, 1HK, 6X, 1HS, 5X, 3HAVO,
15X, 4HCATO, 5X1HH/)84 FORMAT (/3X, I2, 2X, F6.2, 2X, F5.2, 2X, F6.2, 11(2X, F5.2),
12(2X, F6.2), 2X, F5.2)

END

JUNE 18, 1973

EXPERIMENT 1 SIMULATION

FROG 1 CONTROL

JUMP	VO V ₀	TO θ ₀	VW V _w	TW θ _w	Ⓚ Q	I+S I+S	PE Potential E.
1	177.00	52.00	189.16	54.83	1.00	17.01	5.97E 05
2	176.00	58.00	189.04	60.44	1.00	18.99	6.50E 05

JUMP	B F1	M F2	Ⓚ θ'	Ⓜ m	ⓉF t _f	ⓉA t _a	L L	I z	J J
1	39.71	5.90	40.00	6.00	.30	.32	4.90	7.09	2.19
2	35.61	5.98	35.40	6.00	.32	.31	5.22	7.63	2.41

KE Kinetic E.	WD Work Development	PD Power Development	ⓂF mass of frog	ⓂM mass of muscle	Ⓚ Q
1.57E 06	4.51E 05	2.25E 06	100.00	15.00	2.00
1.55E 06	4.73E 05	2.36E 06	100.00	15.00	2.00

A A	E E	C C	K K	S S	AVO approximate V ₀	CATO approximate θ ₀	Ⓚ H
42.00	31.03	33.00	1.97	9.92	198.46	47.82	9.00
37.40	28.42	29.66	1.24	11.36	191.90	54.82	9.00

FROG 2 CONTROL

JUMP	VO	TO	VW	TW	Q	I+S	PE
1	199.00	45.00	208.16	47.47	1.10	16.14	5.10E 05
2	263.00	47.00	268.50	48.09	1.10	25.11	5.32E 05

JUMP	B	M	B	M	TF	TA	L	I	J
1	50.42	5.62	50.00	5.90	.30	.32	4.35	6.04	1.70
2	79.71	6.40	80.00	5.91	.40	.31	4.39	6.25	1.86

KE	WD	PD	MF	MM	D
2.09E 06	5.53E 05	2.76E 06	105.32	14.68	1.85
3.64E 06	9.17E 05	4.59E 06	105.32	14.68	1.85

A	E	C	K	S	AVO	CATO	H
51.85	40.41	41.81	1.40	10.09	222.23	41.43	8.55
81.85	70.41	72.07	1.66	18.86	280.03	44.44	8.55

 FROG 3 EXPER.

JUMP	VO	TO	VW	TW	Q	I+S	PE
1	188.00	49.00	188.40	49.11	.98	16.30	4.90E 05
2	245.00	55.00	245.45	55.07	.98	27.09	5.40E 05

JUMP	B	M	B	M	TF	TA	L	I	J
1	44.27	7.88	44.00	8.00	.29	.33	6.05	6.04	-0.01
2	64.82	7.85	65.00	8.00	.41	.33	6.56	6.55	-0.01

KE	WD	PD	MF	MM	D
1.75E 06	4.50E 05	2.25E 06	99.00	15.10	2.01
2.97E 06	7.05E 05	3.52E 06	99.00	15.10	2.01

A	E	C	K	S	AVO	CATO	H
46.01	35.72	35.52	-0.20	10.26	207.88	43.15	8.00
67.01	57.58	57.83	.26	20.54	255.92	51.75	8.00

FROG 4 EXPER.

JUMP	VO	TO	VW	TW	Q	I+S	PE
1	202.00	41.00	201.78	40.93	1.00	8.95	8.7*F 04
2	210.00	55.00	209.24	54.85	1.00	15.09	8.7*E 04

JUMP	B	M	B	M	TF	TA	L	T	J
1	38.97	.07	39.00	0	.27	.35	0	0	0
2	39.99	.20	40.00	0	.35	.29	0	0	0

KE	WD	PD	MF	MM	D
1.82E 06	2.47E 05	1.23E 06	89.00	20.00	2.20
1.96E 06	3.23E 05	1.62E 06	89.00	20.00	2.20

A	E	C	K	S	AVO	CATO	H
41.20	41.23	41.20	-0.03	8.95	195.88	42.51	0
42.20	42.30	42.20	-0.10	15.09	206.09	56.35	0